ResearchGate

See discussions, stats, and author profiles for this publication at: https://www.researchgate.net/publication/228891679

# Iron in kornerupine: A 57Fe Mossbauer spectroscopic study and comparison with single-crystal structure refinement

**Article** *in* American Mineralogist · April 1999

DOI: 10.2138/am-1999-0407

CITATIONS
11

READS
85

**7 authors**, including:

Edward Grew
University of Maine
**226** PUBLICATIONS **4,793** CITATIONS
SEE PROFILE

Günther J Redhammer
University of Salzburg
**288** PUBLICATIONS **2,334** CITATIONS
SEE PROFILE

Georg Amthauer
University of Salzburg
**512** PUBLICATIONS **3,263** CITATIONS
SEE PROFILE

Frank C Hawthorne
University of Manitoba
**1,170** PUBLICATIONS **23,321** CITATIONS
SEE PROFILE

**Some of the authors of this publication are also working on these related projects:**



Tourmaline in rare-element pegmatites View project



Structure Hierarchy in Minerals View project

All content following this page was uploaded by Günther J Redhammer on 31 May 2014.

The user has requested enhancement of the downloaded file.

*American Mineralogist, Volume 84, pages 536–549, 1999*

# Iron in kornerupine: A $^{57}$Fe Mössbauer spectroscopic study and comparison with single-crystal structure refinement

**Edward S. Grew,[1,*] Günther J. Redhammer,[2] Georg Amthauer,[2] Mark A. Cooper,[3] Frank C. Hawthorne,[3] and Karl Schmetzer[4]**

[1]Department of Geological Sciences, University of Maine, 5790 Bryand Center, Orono, Maine 04469, U.S.A.
[2]Institut für Mineralogie, Universität Salzburg, Hellbrunnerstrasse, 34 A-5020 Salzburg, Austria
[3]Department of Geological Sciences, University of Manitoba, Winnipeg, Manitoba R3T 2N2, Canada
[4]Marbacherstrasse, 22b, D-85238 Petershausen, Germany

## Abstract

Iron is an important constituent of kornerupine, (□,Mg,Fe)(Al,Mg,Fe)$_9$(Si,Al,B)$_5$O$_{21}$(OH,F). We obtained Mössbauer spectra at 300 K on twelve samples with ΣFe = 0.30–1.30 atoms per formula unit (apfu) and Fe$^{3+}$/ΣFe = 0–0.31; several samples were also run at 77 and 430 K. Models allowing unequivocal refinement of the spectra and determination of site occupancies were developed only when single-crystal refinement (SREF) of six of the samples constrained the number of possibilities. The spectra could then be fitted to three Fe$^{2+}$ doublets and one Fe$^{3+}$ doublet. The Fe$^{2+}$doublets have nearly identical isomer shifts: δ = 1.14–1.19 mm/s for the octahedral M1 and M2 sites and 1.12–1.20 mm/s for the irregular, eightfold-coordinated X site (relative to α-Fe at 300 K). However, they differ to a variable extent in quadrupole splitting, $\Delta E_Q \approx$ 1.06–1.80, 1.83–2.27, and 2.14–3.41 mm/s, respectively, to the M1, M2, and X sites. The Fe$^{3+}$ doublet corresponds to the M4 site. The Mössbauer and SREF occupancies are in excellent agreement for the six samples.

The M1 doublet is split in B-bearing kornerupine and the proportion of Fe corresponding to each doublet, as well as quadrupole splitting, varies with B content. Similarly, the X doublet is split in F-bearing kornerupine, and quadrupole splitting of the X site increases with increasing F content. In contrast to most silicates, resolution of the spectra improves with increasing temperature. Quadrupole splitting of the X, M1, and M2 sites decreases with temperature, the X site at a lesser rate consistent with its being the most distorted site.

To a first approximation, the Fe$^{3+}$/ΣFe ratio in kornerupine determined by SREF and Mössbauer spectroscopy increases with increasing $Fe_2O_3$ and Fe$^{3+}$/ΣFe ratio of the associated sillimanite, sapphirine, and ilmenite-hematite, i.e., the measured Fe$^{3+}$/ΣFe ratios are related to the oxygen fugacity at which the kornerupine crystallized.

## Introduction

Kornerupine sensu lato, approximately (□,Mg,Fe)(Al,Mg,Fe)$_9$(Si,Al,B)$_5$O$_{21}$(OH,F), is a mineral group occurring in Mg-Al-rich rocks, magnesian metapelites and, very rarely, pegmatites in upper amphibolite- and granulite-facies terrains; it includes kornerupine sensu stricto ($0 \leq B < 0.5$ apfu) and prismatine ($1 > B > 0.5$ apfu) (Grew et al. 1996). Its complex chemical composition was aptly termed ''formidable'' by Moore and Bennett (1968). Contributing to this complexity is the variation in Fe$^{3+}$/ΣFe ratio, which ranges from 0 to 1, one of the most extensive among ferromagnesian silicates. However, this ratio cannot be measured by electron and ion microprobe analyses; it requires another technique, such as $^{57}$Fe Mössbauer spectroscopy.

This paper reports the results of the Mössbauer spectroscopic study of twelve specimens and their petrologic implications. Unequivocally identifying the sites occupied by Fe is impossible using Mössbauer spectroscopy alone, even with several single-crystal structure refinements (SREF) of kornerupine to use as guides (Moore and Bennett 1968; Moore and Araki 1979; Finger and Hazen 1981; Moore et al. 1989; Klaska and Grew 1991). The spectra were too complex and the possible site assignments too numerous. Therefore, by combining our spectroscopic results with crystallographic data on six specimens (Cooper 1997), we developed models for refining the Mössbauer spectra, identifying the doublet due to Fe at the distorted eightfold-coordinated X site, and deducing site occupancies that agree remarkably well with the crystallographic data. The Fe in these 12 kornerupines is predominantly ferrous. Spectra were also obtained from a specimen (no. 128415, Bjordam, Bamble, Norway, and van der Wel 1973) that contains more Fe$^{3+}$

* E-mail: esgrew@maine.maine.edu

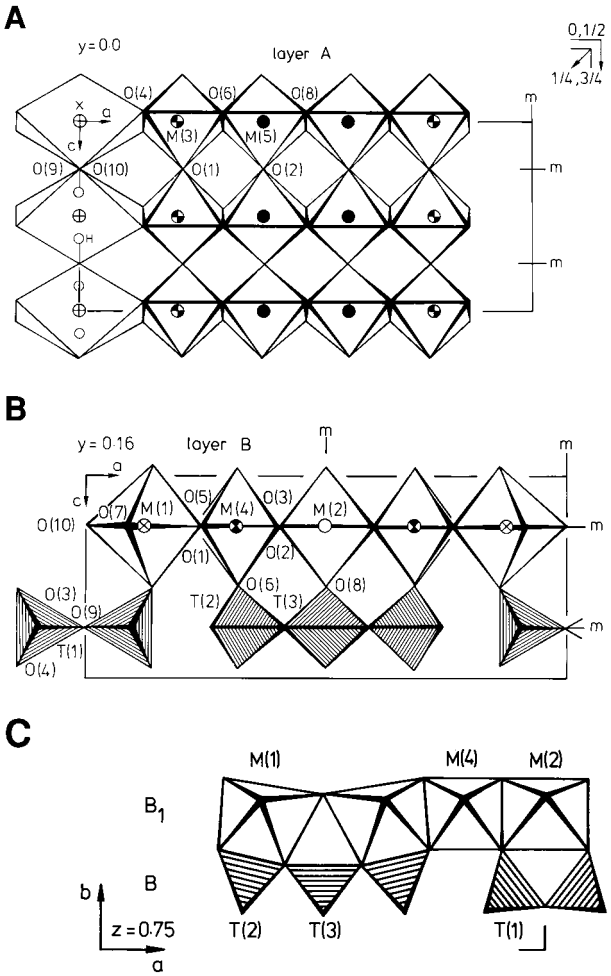


**FIGURE 1.** Elements of the structure of kornerupine. (**a**) Projection parallel to [010] of the A layer in kornerupine at $y = 0$, (**b**) Projection parallel to [010] of the B layer in kornerupine at $y = 0.16$, (**c**) Projection parallel to [001] of a part of the kornerupine structure at $z = 0.75$ [Used by permission from Klaska and Grew (1991), Figs. 1–3, modified by combining into one figure].

than $Fe^{2+}$. We did not succeed in finding a model to refine its spectrum, which may include features from secondary hematite, an impurity present in this specimen (Grew et al. 1990). Cooper (1997) also was not able to get satisfactory agreement between Fe from electron microprobe analysis and Fe from SREF for the ferrian kornerupines from Bjordam and, consequently, its Mössbauer spectrum is not reported here.

## Kornerupine crystal chemistry

Kornerupine is orthorhombic, space group *Cmcm*. Moore and Araki (1979) preferred to describe its dense, but only locally cubic closed-packed, structure on the basis of two kinds of sheets, A and B, which alternate ABBABBA (Fig. 1). There are nine sites in kornerupine (Table 1). The most notable feature of the tetrahedra, which occur as dimers and trimers, is the variable B content of T3, which is coupled with Si content in T2: $^{[T3]}B + {}^{[T2]}Si \leftrightarrow {}^{[T3]}Si + {}^{[T2]}Al$.

**TABLE 1.** Major element cation site-occupancies

| Octahedral | | Tetrahedral | |
|---|---|---|---|
| Site | Atom | Site | Atom |
| M1 | Mg, $Fe^{2+}$ | T1 | Si, Al |
| M2 | Mg, Al, $Fe^{2+}$ | T2 | Si, Al |
| M3 | Al, Mg | T3 | Si, B, Al |
| M4 | Al, Mg, $Fe^{3+}$ | | [8]-coordinated |
| M5 | Al, Mg | X | □, $Fe^{2+}$, Mg, Na |

*Note:* □ denotes vacancy. Multiplicities are 4 for M2, T3 and X. All other sites have multiplicities of 8. From crystal structure determination (e.g., Moore et al. 1989; Cooper 1997).

Moore and Araki (1979) reported that, in a synthetic Fe-free kornerupine, M1 and M4 are the most distorted of the octahedral sites, whereas M3 and M5 are the least distorted. M1 is unique among the octahedra in sharing an edge with a tetrahedron, T2.

OH and F have been definitively located at O10 only. Cooper (1997) concluded that no O is present at this site, and thus kornerupine formulae can be normalized on the basis of 43 anionic charges. In addition to the cations listed above, Li, Be, Ca, Ti, V, Cr, and Mn also have been reported, but only in minor amounts (e.g., Grew et al. 1990; Grew 1996; Cooper 1997).

## Sample preparation and composition

Samples (Table 2) were separated from rock by hand (nos. 1, 3, 7, 8, and 12, Grew et al. 1990) or by conven-

**TABLE 2.** List of kornerupine samples studied by Mössbauer spectroscopy

| No. | Locality and Reference | Original sample number | Cooper (1997) number |
|---|---|---|---|
| 1 | Sinyoni Claims, Zimbabwe*‡§‖ | 9365 | K35 |
| 2 | Sinyoni Claims, Zimbabwe*‡ | 9371 | — |
| 3 | Ellammankovilpatti, India‖# | 3083D | K1 |
| 4 | Sinyoni Claims, Zimbabwe† | 8497 | K22 |
| 5 | Ampanihy, Madagascar (Gemstone) | P559 | — |
| 6 | Madagascar (Gemstone) | P560 | — |
| 7 | Madagascar‖ | 171.350 | K7 |
| 8 | Madagascar‖ | 141255 | K9 |
| 9 | Sri Lanka (Gemstone) | P676 | — |
| 10 | Waldheim, Germany | P540 | — |
| 11 | Lac Ste. Marie, Quebec, Canada | P539 | — |
| 12 | Port Shepstone, South Africa‖ ** | BM1940,39 | K11 |

*Note:* Grew (1996) reviews the literature on the localities listed here.

* These two specimens donated by W. Schreyer are derived from a single block about 25 cm across (Schreyer, personal communication, 1998). We received one specimen, which is presumably no. 9371, in 1976 or 1977, and the second, no. 9365, in 1983.

† Sample no. 3 (8497) is a coarse kornerupine prism in a matrix of cordierite, sillimanite, and phlogopite; kyanite occurs as rare, rounded relics in kornerupine. In contrast to the B-free kornerupine (no. 1), there is no evidence of kornerupine breakdown.

‡ Schreyer and Abraham (1976).

§ Klaska and Grew (1991).

‖ Grew et al. (1990).

# Grew (1982), Grew et al. (1987a).

** de Villiers (1940); Hey et al. (1941).

**TABLE 3.** Compositions of kornerupine

| Sample no. | 1* | 2† | 3* | 4* | 5‡ | 7* | 8* | 9§ | 10‖ | 11§ | 12* |
|---|---|---|---|---|---|---|---|---|---|---|---|
| Species | Krn | Krn | Krn | Krn | Prs | Prs | Prs | Prs | Prs | Prs | Prs |
| **Electron-microprobe analyses, $Fe_2O_3$ by SREF, wt%** | | | | | | | | | | | |
| $SiO_2$ | 28.66 | 28.7 | 29.97 | 30.84 | 30.7 | 31.63 | 30.89 | 29.95 | 30.59 | 30.05 | 29.10 |
| $TiO_2$ | 0.12 | 0.11 | 0.12 | 0 | 0.10 | 0 | 0 | — | 0.24 | — | 0.21 |
| $Al_2O_3$ | 48.04 | 47.1 | 44.06 | 44.76 | 39.6 | 40.56 | 40.11 | 42.10 | 42.36 | 41.87 | 41.35 |
| $V_2O_3$ | 0 | — | 0 | 0 | — | 0 | 0 | — | 0.09 | — | 0 |
| $Cr_2O_3$ | 0 | — | 0 | 0 | — | 0 | 0 | — | 0.08 | — | 0 |
| $Fe_2O_3$ | 0.60 | 0.15 | 0.73 | 0.09 | 0.46# | 0.52 | 0.60 | 0.26# | 0.28# | 1.02# | 0 |
| FeO | 2.71 | 4.46 | 3.80 | 1.21 | 2.54 | 2.83 | 4.26 | 4.98 | 6.11 | 8.49 | 12.09 |
| MnO | 0 | 0 | 0 | 0 | 0 | 0 | 0.13 | — | 0.08 | — | 0.12 |
| MgO | 17.72 | 16.2 | 17.32 | 19.35 | 20.0 | 19.20 | 18.05 | 17.98 | 14.53 | 13.41 | 10.81 |
| CaO | 0.08 | 0.07 | 0 | 0 | 0.04 | 0 | 0 | — | 0 | — | 0 |
| $Na_2O$ | 0 | — | 0.04 | 0 | 0.03 | 0 | 0.05 | 0.10 | 0.09 | 0.05 | 0.05 |
| $K_2O$ | 0 | — | 0 | 0 | 0 | 0 | 0 | — | 0 | — | 0 |
| F | 0.02 | — | 0.07 | 0 | — | 0.30 | 0.38 | — | 0.67 | — | 0.85 |
| **Wet-chemical analysis for $Li_2O$, BeO. SREF for $B_2O_3$, except no. 2 (wet chem.) and no. 10 (SIMS), wt%** | | | | | | | | | | | |
| $Li_2O$ | 0 | — | 0.02 | — | — | 0.02 | 0.035 | — | 0.12 | — | 0.19 |
| BeO | 0 | — | 0.01 | — | — | 0.001 | 0.005 | — | 0.003 | — | 0.022 |
| $B_2O_3$ | 0.09 | 0 | 1.88 | 1.99 | — | 3.56 | 3.96 | — | 3.26 | — | 3.89 |
| **Calculated, wt%** | | | | | | | | | | | |
| $H_2O$ | 1.19 | 1.18 | 1.17 | 1.23 | — | 1.08 | 1.03 | — | 0.88 | — | 0.77 |
| O=F | −0.01 | — | −0.03 | 0 | — | −0.13 | −0.16 | — | −0.28 | — | −0.36 |
| Total | 99.22 | 97.97 | 99.16 | 99.46 | 93.47 | 99.58 | 99.35 | 95.37 | 99.10 | 94.89 | 99.10 |
| **Formulae per 21 O atoms and 1 OH, F** | | | | | | | | | | | |
| Si | 3.580 | 3.652 | 3.730 | 3.769 | — | 3.869 | 3.811 | — | 3.817 | — | 3.722 |
| B | 0.020 | 0 | 0.404 | 0.420 | — | 0.752 | 0.844 | — | 0.702 | — | 0.860 |
| Al | 7.073 | 7.064 | 6.463 | 6.447 | — | 5.847 | 5.832 | — | 6.229 | — | 6.234 |
| Ti | 0.011 | 0.011 | 0.011 | 0 | — | 0 | 0 | — | 0.023 | — | 0.020 |
| V | 0 | — | 0 | 0 | — | 0 | 0 | — | 0.009 | — | 0 |
| Cr | 0 | — | 0 | 0 | — | 0 | 0 | — | 0.008 | — | 0 |
| $Fe^{3+}$ | 0.056 | 0.014 | 0.068 | 0.008 | — | 0.048 | 0.056 | — | 0.026 | — | 0 |
| $Fe^{2+}$ | 0.283 | 0.475 | 0.396 | 0.124 | — | 0.290 | 0.440 | — | 0.638 | — | 1.293 |
| Mn | 0 | 0 | 0 | 0 | — | 0 | 0.014 | — | 0.008 | — | 0.013 |
| Mg | 3.300 | 3.073 | 3.214 | 3.525 | — | 3.501 | 3.320 | — | 2.703 | — | 2.061 |
| Ca | 0.011 | 0.010 | 0 | 0 | — | 0 | 0 | — | 0 | — | 0 |
| Na | 0 | — | 0.010 | 0 | — | 0 | 0.012 | — | 0.022 | — | 0.012 |
| Sum | 14.334 | 14.298 | 14.296 | 14.293 | — | 14.307 | 14.329 | — | 14.184 | — | 14.217 |
| F | 0.008 | — | 0.028 | 0 | — | 0.116 | 0.148 | — | 0.264 | — | 0.344 |
| OH | 0.992 | 1.000 | 0.972 | 1.000 | — | 0.884 | 0.852 | — | 0.736 | — | 0.656 |
| $X(Fe^{2+})$ | 0.079 | 0.134 | 0.110 | 0.034 | 0.066 | 0.076 | 0.117 | 0.134 | 0.191 | 0.262 | 0.386 |

*Notes:* Km-kornerupine sensu stricto, Prs-prismatine. 0—at or below limit of detection. Dash (—) not sought or not calculated. In the absence of a B determination, identification of Prs was inferred from low contents of $Al_2O_3$ and other trivalent cations. $Fe_2O_3$ calculated from SREF, except for 5, 9, 10, and 11, where Mössbauer data were used (indicated by #). To maintain consistency with crystal-structure refinements, Li and Be were not included in formula calculations. $X(Fe^{2+}) = Fe^{2+}/(Fe^{2+} + Mg)$. Sources of data:

* Cooper (1997), except $Li_2O$ and BeO from Grew et al. (1990).

† Schreyer and Abraham (1976, Table 1, col. 4), analysis from the margin and may differ from material in the core, which would have been the source of material studied by Mössbauer spectroscopy (Schreyer, personal communication, 1998).

‡ M. Bernroider, analyst, Universität Salzburg.

§ K. Schmetzer, analyst, at Universität Heidelberg.

‖ Average of 4 grains by Ron Chapman at the University of Manitoba, and of two of these grains for $Li_2O$, BeO and $B_2O_3$ by E.S. Grew, C.K. Shearer, and M. Wiedenbeck.

tional techniques (nos. 10 and 11); other samples were simply broken from larger fragments (nos. 2 and 4) or from cut gemstones (nos. 5, 6, and 9).

The kornerupines span the range of composition reported for the kornerupine group in terms of F, B, total Fe, and $Fe^{2+}/(Fe^{2+} + Mg)$ (Table 3; cf. Grew et al. 1990; Grew 1996; Cooper 1997). The samples vary in the extent of chemical homogeneity. Of the samples for which several analyses are available, nos. 7, 8, and 12 are relatively homogeneous (Grew et al. 1990), whereas nos. 1 and 2 vary somewhat in Fe/Mg ratio (Schreyer and Abraham 1976) and nos. 3 and 10 vary in Al as well as Fe and Mg. In no. 10 (Waldheim), the variations from one grain to another are moderate (Fe as FeO = 6.07–6.76, $Al_2O_3$ = 41.71–42.96, MgO = 14.24–14.76 wt%, and F = 0.47–0.84 wt% for 4 grains), and the average is tabulated in Table 3. In no. 3 (India), Fe as FeO = 4.46–7.95, $Al_2O_3$ = 44.80–42.90, and MgO = 17.33–14.98 wt% (Grew 1982; Grew et al. 1990; Cooper 1997); the lower Fe and higher Al values apply to a larger prism similar to that used for Mössbauer spectroscopy as well as to the crystal studied by X-ray diffraction (XRD) (Table 3). The variations in sample 3 could reflect $Al \leftrightarrow Fe^{3+}$ and $Mg \leftrightarrow Fe^{2+}$ substitution; the sample is reasonably homogeneous in B.

The unanalyzed sample (no. 6 or P560) could be pris-

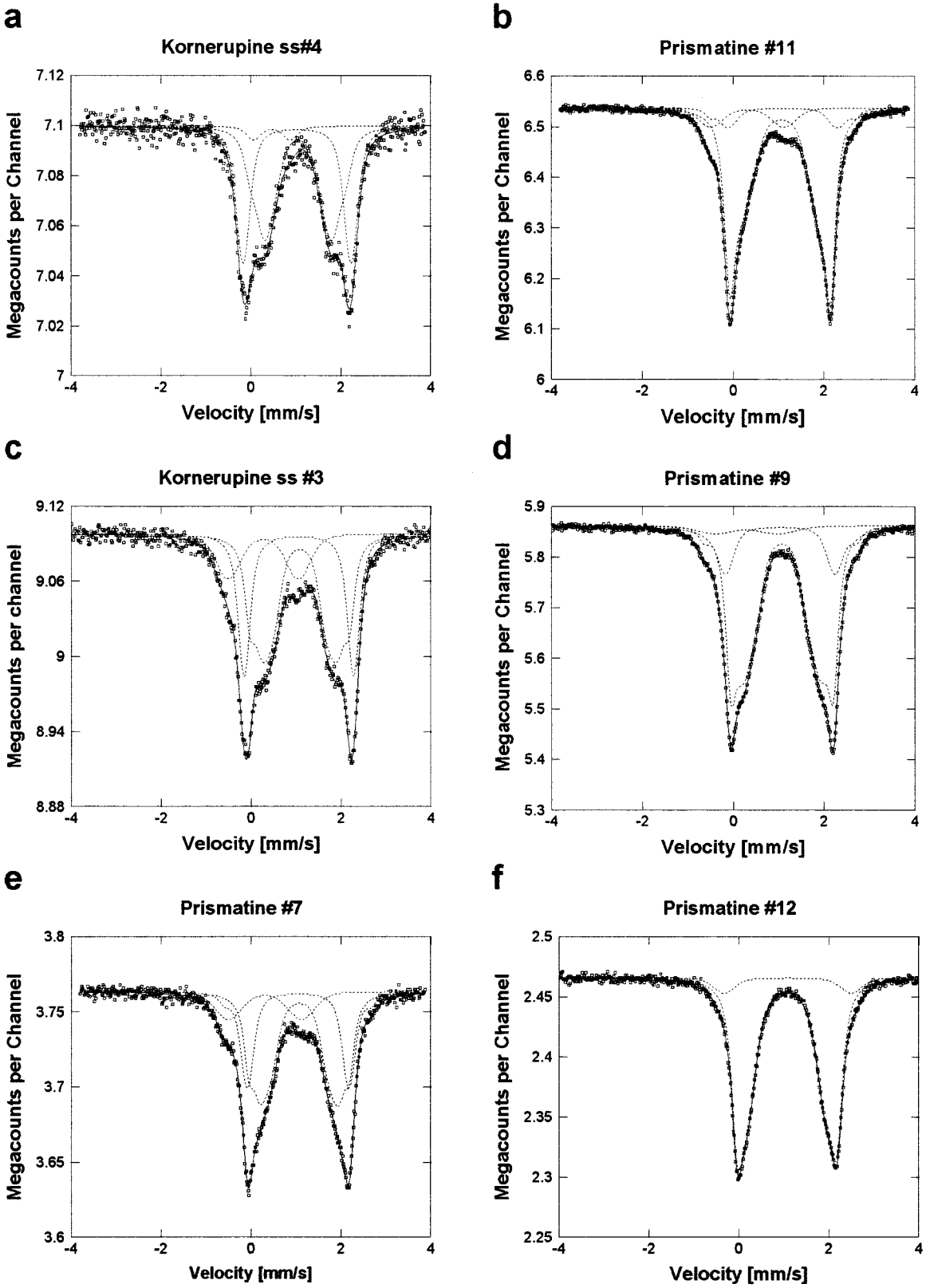


**FIGURE 2.** Typical $^{57}$Fe Mössbauer spectra of kornerupine sensu stricto (ss) and prismatine recorded at 300 K and atmospheric pressure.

**TABLE 4.** List of $^{57}$Fe hyperfine fit parameters

| | | Split M1-inner | | | | Split M1-outer | | | | M2 site | | | |
|---|---|---|---|---|---|---|---|---|---|---|---|---|---|
| Sample | $T$ | δ | σ | $\Delta E_Q$ | $A_{rel}$ | δ | σ | $\Delta E_Q$ | $A_{rel}$ | δ | σ | $\Delta E_Q$ | $A_{rel}$ |
| 1. Sinyoni | 77 | — | — | — | — | 1.304 | 0.134 | 2.252 | 29.3 | 1.302 | 0.593 | 2.383 | 10.5 |
| | 300 | — | — | — | — | 1.142 | 0.305 | 1.299 | 34.7 | 1.132 | 0.172 | 1.894 | 9.6 |
| | 430 | — | — | — | — | 1.067 | 0.236 | 0.965 | 33.7 | 1.063 | 0.16* | 1.638 | 10.4 |
| 2. Sinyoni | 300 | — | — | — | — | 1.152 | 0.313 | 1.264 | 26.2 | 1.167 | 0.359 | 1.826 | 29.1 |
| 3. India | 300 | 1.181 | 0.182 | 1.088 | 10.7 | 1.181 | 0.301 | 1.633 | 31.4 | 1.181 | 0.07* | 2.229 | 10.7 |
| 4. Sinyoni | 300 | 1.155 | 0.253 | 1.114 | 16.1 | 1.154 | 0.212 | 1.539 | 25.6 | 1.153 | 0.172 | 2.10* | 11.3 |
| | 430 | — | — | — | — | 1.049 | 0.20* | 1.041 | 41.8 | 1.049 | 0.20* | 1.477 | 10.3 |
| 5. Madagascar | 300 | 1.162 | 0.272 | 1.253 | 22.3 | 1.174 | 0.113 | 1.586 | 15.4 | 1.197 | 0.067 | 2.203 | 13.0 |
| 6. Madagascar | 300 | 1.198 | 0.192 | 1.287 | 16.7 | 1.197 | 0.164 | 1.793 | 23.8 | 1.197 | 0.041 | 2.181 | 4.9 |
| 7. Madagascar | 300 | 1.175 | 0.251 | 1.313 | 23.1 | 1.173 | 0.172 | 1.796 | 19.6 | 1.170 | 0.056 | 2.244 | 13.2 |
| 8. Madagascar | 77 | 1.253 | 0.364 | 1.461 | 18.2 | 1.268 | 0.159 | 1.961 | 15.8 | 1.299 | 0.262 | 2.914 | 20.2 |
| | 300 | 1.163 | 0.272 | 1.295 | 22.3 | 1.163 | 0.113 | 1.693 | 12.7 | 1.163 | 0.067 | 2.24* | 15.9 |
| 9. Sri Lanka | 77 | 1.300 | 0.472 | 2.150 | 14.4 | 1.308 | 0.060 | 2.418 | 27.4 | 1.316 | 0.331 | 2.713 | 36.5 |
| | 300 | 1.170 | 0.181 | 1.064 | 9.5 | 1.177 | 0.330 | 1.696 | 45.0 | 1.180 | 0.067 | 2.266 | 23.9 |
| 10. Waldheim | 77 | 1.296 | 0.356 | 2.104 | 5.8 | 1.302 | 0.10* | 2.442 | 45.2 | 1.312 | 0.372 | 2.785 | 23.5 |
| | 300 | 1.159 | 0.096 | 0.995 | 3.0 | 1.148 | 0.308 | 1.682 | 44.8 | 1.140 | 0.072 | 2.213 | 28.8 |
| | 430 | — | — | — | — | 1.086 | 0.376 | 1.470 | 46.9 | 1.094 | 0.118 | 2.064 | 27.1 |
| 11. Quebec | 300 | 1.173 | 0.192 | 1.144 | 7.5 | 1.156 | 0.276 | 1.741 | 33.6 | 1.143 | 0.077 | 2.230 | 39.6 |
| 12. Shepstone | 300 | 1.149 | 0.440 | 1.187 | 6.3 | 1.162 | 0.274 | 1.768 | 48.8 | 1.172 | 0.104 | 2.224 | 36.7 |

*Note:* All spectra imply a Lorentzian width of 0.24 mm/s. δ = isomer shift [mm/s] relative to α-Fe ± 0.02 mm/s, $\Delta E_Q$ = quadrupole splitting [mm/s] ± 0.03 mm/s, σ = Gaussian width of the absorption lines [mm/s] ± 0.04 mm/s and $A_{rel}$ = relative area ratio [percentage] of Fe on a specific position compared to total Fe ± 2%. These errors are estimated on basis of the calculated ones, which range between 0.009–0.031 mm/s for isomer shifts, between 0.011–0.034 mm/s for $\Delta E_Q$, between 0.03 and 0.05 mm/s for σ and between 0.9 and 2.1% for area ratios.

* Parameter fixed during final refinement.

matine, as are most other specimens from Madagascar (Grew 1996).

## EXPERIMENTAL METHODS

Transmission $^{57}$Fe Mössbauer spectra were collected with a conventional spectrometer (Halder Electronic GmbH, Germany) in the horizontal arrangement using a ~50 mCi $^{57}$Co/Rh matrix single-line thin source, an electromechanical drive-system with constant acceleration and symmetric triangular velocity-shape, and a multichannel analyzer with 1024 channels. The velocity range was ±4 mm/s and the spectrometer velocity was regularly calibrated with a thin high-purity α-Fe foil. Isomer-shift values δ are given relative to the α-Fe standard. The spectra for all 12 samples were recorded at 300 K (room temperature). Additional spectra for five samples were collected at 77 K using liquid nitrogen and a bath cryostat for cooling. Spectra of three samples were also recorded at 430 K using a heating device designed in-house.

The two symmetric spectra obtained (512 channels each) were calibrated, folded, and analyzed using the Voigt-based quadrupole splitting distribution (QSD) method (Rancourt and Ping 1991; Ping et al. 1991; Rancourt et al. 1994a, 1996). The method uses a certain number *m* of generalized sites each having its own continuous QSD, built up by a certain number of *n* Gaussian components. The QSD analysis requires the following fitting parameters (Rancourt et al. 1996): (1) two spectrum-specific parameters (BG = background, Γ = the Lorentzian width of the lines); (2) two site specific parameters, $\delta_0$ and $\delta_1$; (3) three component-specific parameters, h, the height of one line in the symmetric elemental Lorentzian doublet and the position or center of the Gaussian QSD component; and (4) σ, the σ-width of the Gaussian QSD component. The isomer shifts are assumed to be correlated to their quadrupole splittings (QS, $\Delta E_Q$) as $\delta = \delta_o + \delta_1 \Delta E_Q$. In analyzing the spectra, the Lorentzian width Γ was constrained to be the same value for all generalized sites value: 0.24 mm/s. This value was found in the Salzburg laboratory to be typical for silicates, e.g., clinopyroxenes, garnets, without using the QSD method.

## RESULTS

The main feature of all the spectra are two dominant more or less asymmetrically broadened resonance-absorption peaks centered on zero velocity (0.00 mm/s) and 2.15 mm/s (Fig. 2). We refined the spectra using a model with three generalized sites with up to three components each. The dominant absorption peaks result from superposition of at least two symmetric components that can be assigned to $Fe^{2+}$. The $Fe^{2+}$ contribution was refined with two sites, one having one to two components and being assigned to the X site, and the second one having two to three components and being a generalized site for octahedral $Fe^{2+}$. Additionally, several spectra show distinct shoulders centered around 0.5 and 1.15 mm/s, which can be fitted by one symmetric quadrupole doublet. On the basis of the $^{57}$Fe hyperfine parameters, this doublet can be assigned to $Fe^{3+}$, which Moore et al. (1989) and Cooper (1997) located at the M4 site.

The spectra fall into a Fe-poor group with $X(Fe^{2+}) = Fe^{2+}/(Fe^{2+} + Mg) < 0.12$ (nos. 1–8; e.g., Figs. 2a, 2c, and 2e) and an Fe-rich group, $X(Fe^{2+}) > 0.12$ (nos. 9–12; Figs. 2b, 2d, and 2f). The Fe-poor spectra are rich in detail, whereas the Fe-rich spectra show less distinct shoulders and asymmetric broadening of the absorption lines. We begin our discussion with the Fe-poor kornerupines sensu stricto, which were used to develop the models.

**TABLE 4—***Continued*

| X-site | | | | X′-site | | | | $Fe^{3+}$ at M4 | | | | |
|---|---|---|---|---|---|---|---|---|---|---|---|---|
| δ | σ | $\Delta E_Q$ | $A_{rel}$ | δ | σ | $\Delta E_Q$ | $A_{rel}$ | δ | σ | $\Delta E_Q$ | $A_{rel}$ | $\chi^2$ |
| 1.297 | 0.153 | 2.619 | 46.1 | — | — | — | — | 0.456 | 0.70* | 1.727 | 14.1 | 2.492 |
| 1.117 | 0.094 | 2.483 | 39.4 | — | — | — | — | 0.351 | 0.448 | 1.677 | 16.3 | 2.255 |
| 1.060 | 0.127 | 2.359 | 37.3 | — | — | — | — | 0.254 | 0.563 | 1.598 | 18.7 | 2.337 |
| 1.138 | 0.178 | 2.403 | 41.6 | — | — | — | — | 0.435 | 0.20* | 0.798 | 3.0 | 2.089 |
| 1.162 | 0.140 | 2.43* | 30.6 | — | — | — | — | 0.371 | 0.430 | 1.558 | 16.6 | 2.158 |
| 1.127 | 0.171 | 2.397 | 42.6 | — | — | — | — | 0.463 | 0.20* | 0.814 | 4.4 | 1.693 |
| 1.033 | 0.158 | 2.229 | 40.2 | — | — | — | — | 0.303 | 0.15* | 0.469 | 7.7 | 2.142 |
| 1.150 | 0.265 | 2.164 | 35.3 | — | — | — | — | 0.440 | 0.403 | 1.641 | 14.0 | 2.005 |
| 1.173 | 0.099 | 2.257 | 21.3 | 1.203 | 0.99 | 3.409 | 2.6 | 0.447 | 0.587 | 1.731 | 30.7 | 2.013 |
| 1.146 | 0.164 | 2.259 | 27.6 | 1.146 | 0.094 | 3.243 | 2.2 | 0.411 | 0.502 | 1.625 | 14.3 | 1.843 |
| 1.300 | 0.134 | 2.429 | 31.9 | — | — | — | — | 0.418 | 0.405 | 1.807 | 13.9 | 2.159 |
| 1.148 | 0.223 | 2.142 | 29.7 | 1.148 | 0.158 | 3.197 | 1.7 | 0.384 | 0.406 | 1.689 | 17.7 | 2.077 |
| 1.237 | 0.278 | 2.765 | 13.4 | 1.262 | 0.05* | 3.762 | 2.6 | 0.507 | 0.687 | 1.283 | 5.7 | 2.012 |
| 1.141 | 0.246 | 2.406 | 14.2 | 1.141 | 0.122 | 3.345 | 2.9 | 0.386 | 0.705 | 1.379 | 4.5 | 2.460 |
| 1.270 | 0.239 | 2.749 | 17.9 | 1.270 | 0.07* | 3.815 | 2.9 | 0.455 | 0.80* | 1.431 | 4.7 | 2.089 |
| 1.154 | 0.212 | 2.392 | 14.9 | 1.154 | 0.161 | 3.191 | 4.5 | 0.487 | 0.541 | 1.079 | 4.0 | 1.890 |
| 1.075 | 0.369 | 2.25* | 21.3 | — | — | — | — | 0.365 | 0.888 | 1.313 | 4.7 | 2.100 |
| 1.201 | 0.273 | 2.397 | 7.6 | 1.201 | 0.039 | 3.207 | 1.9 | 0.424 | 0.429 | 1.613 | 9.8 | 2.320 |
| 1.185 | 0.206 | 2.669 | 5.8 | 1.292 | 0.121 | 3.22 | 2.3 | — | — | — | — | 1.966 |

One of the key samples for spectral refinements is the B-free kornerupine from Sinyoni Claims (no. 1) (Fig. 3). In contrast to the spectra for prismatine, the $Fe^{2+}$ absorption in no. 1 is clearly split into two distinct doublets. Nonetheless, refinement with two $Fe^{2+}$ components for these two peaks gave unsatisfactory results because the asymmetry of the inner peaks was not satisfactorily modeled. This is clear evidence that the inner peak is a superposition of two components. Refinements with three $Fe^{2+}$ components and one $Fe^{3+}$ component led to excellent agreement between the experimental and calculated spectra (Fig. 3c). The three components have nearly identical isomer shifts (1.12–1.14 mm/s at 300 K) but differ significantly in quadrupole splitting, 1.30, 1.89, and 2.48 mm/s (Table 4). These values are consistent with octahedrally coordinated $Fe^{2+}$. Comparably low values (1.5 mm/s) have been reported for highly distorted sites in certain trioctahedral micas, notably fluorannite (Dyar and Burns 1986; Rancourt et al. 1996; Redhammer 1998). Rancourt et al. (1994b) attributed low $\Delta E_Q$ values to the distorted ''defect site $Fe^{2+}$'' in synthetic annite. However, single-crystal structure refinement of this sample show that $Fe^{2+}$ occupies not only the octahedral M1 and M2 sites, but also the strongly distorted X site, which is eightfold coordinated (Klaska and Grew 1991; Cooper 1997). Ferrous iron at dodecahedral sites should have somewhat larger isomer shift (δ) and quadrupole splitting ($\Delta E_Q$) values than those observed in sample 6 (Amthauer et al. 1976). Because there are no signs of resonance absorption with larger splittings than those of the outer doublet with $\Delta E_Q$ = 2.48 mm/s and because quadrupole splitting for $Fe^{2+}$ is negatively correlated with polyhedral distortion for a given site, we assign the outermost $Fe^{2+}$ doublet to the strongly distorted X site (cf. $\Delta E_Q$ near 3.5 mm/s for a more typical eightfold-coordinated site, e.g., garnet, Amthauer et al. 1976). The two inner doublets can undoubtedly be assigned to $Fe^{2+}$ iron in sixfold coordination; the doublet with the higher quadrupole splitting corresponds to the least distorted octahedron (Hawthorne 1988). Thus the doublet with $\Delta E_Q$ =1.89 mm/s is assigned to $Fe^{2+}$ in the less distorted M2 octahedron, and the doublet with $\Delta E_Q$ =1.30 mm/s is assigned to $Fe^{2+}$ at the M1 site. There is strong support for this assignment in the good agreement between the area—ratios of the spectral bands and the site populations derived by SREF (Table 5). On the basis of the area ratios, no other site assignment is possible. Only the relative area ratios measured at 77 K differ slightly from X-ray structure refinement results.

Refinement of the spectrum for no. 2, which is a B-free konerupine from the same block as no. 1 (Schreyer, personal communication), yields nearly the same hyperfine parameters as for no. 1 (Table 4), although in appearance, the spectrum resembles that of no. 4 (Fig. 2a, see below).

Separation of the $Fe^{2+}$ absorption arising from the doublet with highest splitting (X site) and those of the M sites is also pronounced in the spectrum of kornerupine sensu stricto from Ellammankovilpatti, India, no. 3, sample 3083D (Fig. 2c), although to a lesser degree than in the B-free kornerupine. At first, the spectrum was refined with one site having one component for $Fe^{3+}$ at the M4 site, one site having one component for the X site and one site with two components for the octahedral sites. The component for the X site is just as clearly separated from the octahedral $Fe^{2+}$ QSD as in the case of the B-free kornerupine. However, there is a distinct asymmetric broadening of the M1 doublet in the spectrum of the kornerupine sensu stricto from India. The misfit seems to occur between 0.5 and 1.0 mm/s. Thus, a second $Fe^{2+}$ component was introduced in order to account for this asymmetric distribution. In summary, if we assume that $Fe^{2+}$ at M1 has two different local environments (thereby giving rise to two quadrupole-split doublets), and also occupies a regular M2 site and the X site, we obtain a perfect fit to the experimental data. Moreover, the relative

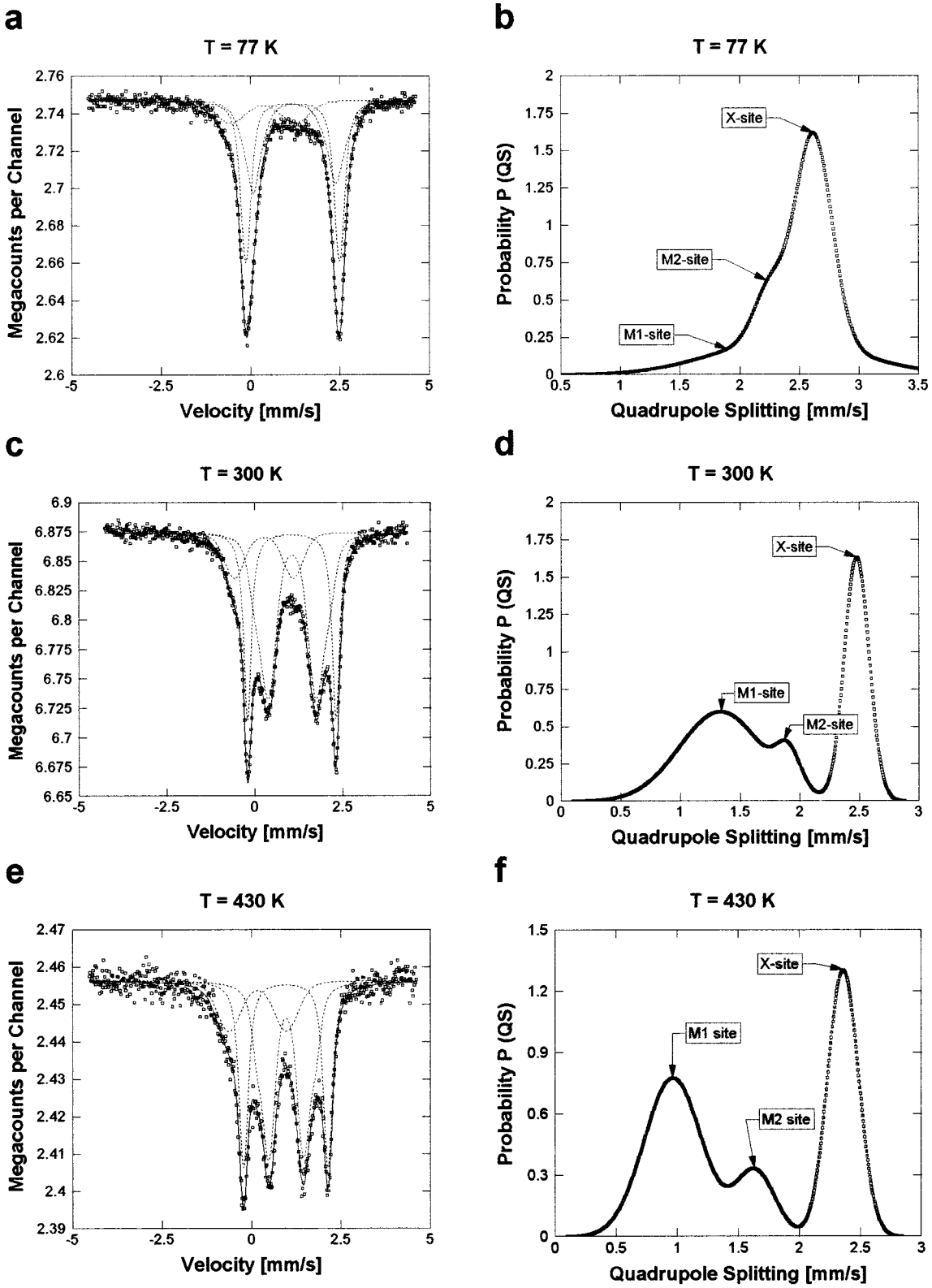


**FIGURE 3.** $^{57}$Fe Mössbauer spectra at 77, 300, and 430 K of the B-free kornerupine (no. 1, sample 9365) with corresponding quadrupole-splitting distributions for $Fe^{2+}$.

**TABLE 5.** Comparison between relative site occupations of total Fe (percent) as derived from single-crystal structure refinement (Cooper 1997) and Mössbauer spectroscopy (this study)

| Sample | Method | T, K | X | M1 | M2 | M4 |
|---|---|---|---|---|---|---|
| 1. Sinyoni | SREF | 300 | 41.9 | 34.2 | 7.4 | 16.5 |
| | Mössbauer | 77 | 46.1 | 29.3 | 10.5 | 14.1 |
| | Mössbauer | 300 | 39.4 | 34.7 | 9.6 | 16.3 |
| | Mössbauer | 430 | 37.3 | 33.7 | 10.4 | 18.7 |
| 3. India | SREF | 300 | 31.7 | 43.1 | 10.6 | 14.7 |
| | Mössbauer | 300 | 30.6 | 42.1 | 10.7 | 16.6 |
| 4. Sinyoni | SREF | 300 | 37.9 | 45.5 | 10.6 | 6.1 |
| | Mössbauer | 300 | 42.6 | 41.7 | 11.3 | 4.4 |
| | Mössbauer | 430 | 40.2 | 41.8 | 10.3 | 7.7 |
| 7. Madagascar | SREF | 300 | 29.3 | 40.2 | 16.3 | 14.2 |
| | Mössbauer | 300 | 29.8 | 42.7 | 13.2 | 14.3 |
| 8. Madagascar | SREF | 300 | 35.3 | 37.1 | 16.3 | 11.3 |
| | Mössbauer | 77 | 31.9 | 34.0 | 20.2 | 13.9 |
| | Mössbauer | 300 | 31.4 | 35.0 | 15.9 | 17.7 |
| 12. Shepstone | SREF | 300 | 9.2 | 54.8 | 36.0 | 0 |
| | Mössbauer | 300 | 8.1 | 55.1 | 36.7 | 0 |

areas of Fe at the four possible sites are in excellent agreement with single-crystal X-ray data (Table 5).

Splitting of the M1 doublet into two doublets differing markedly in $\Delta$ could be due to the presence of B in kornerupine sensu stricto no. 3. The B-bearing T3 tetrahedron shares corners with the M1 octahedron (Fig. 1). Substitution of the small B cation for the larger Al and Si cations on T3 (and concomitant Si $\rightarrow$ Al substitution at T2, which shares an edge with M1) would alter the geometry of the M1 octahedron, giving rise to changes in quadrupole splitting (see below).

Because of the low $Fe_{tot}$ content (1.28 wt% as FeO, Table 3) in kornerupine sensu stricto from Sinyoni Claims (no. 4), its spectrum is noisy and there is significant uncertainty in the hyperfine parameters. Nonetheless, the spectrum shows the same features as the spectrum of no. 3 (Figs. 2a and 2c). There is good separation of the absorptions from $Fe^{2+}$ at the X site and the M sites. The doublet for M1 site is split into two doublets differing in quadrupole splitting, which we attribute to the effect of B at T3.

The spectrum of Sinyoni Claims kornerupine sensu stricto (no. 4) taken at 430 K also shows a distinct separation of the X-site absorption from the M-site absorption. Although relatively broad, the M1 doublet for no. 3 at 430 K shows little asymmetry and splitting it into two components is not necessary. Overall, the relative area ratios of Fe at the different sites could be determined with high precision in the 430 K spectrum and they agree well with the single-crystal X-ray refinement values (Table 5).

In spectra of prismatine (Fig. 2) the X-site doublet is less separated from the M-site doublets than is the case in kornerupine sensu stricto. Nonetheless, the model applied to nos. 2 and 3 was used successfully to refine the spectra of prismatine and those samples inferred to be prismatine from their low content of trivalent cations (Table 3). In most cases, close agreement was achieved between relative area-ratios of Fe as derived by Mössbauer spectroscopy and single-crystal structure refinements (Table 5). The absorptions from Fe at the X and the M2 sites overlap to such an extent in the spectra of the four prismatines from Madagascar that the relative area-ratios of Fe at the X site were constrained to the SREF values during the fitting process and were released only in the final calculations. Doing so, it was possible to obtain close agreement for these samples. Due to the relatively high proportion of $Fe^{2+}$ at the M2 site in the Fe-rich samples, the M1 and M2 doublets are more nearly superimposed and the total $Fe^{2+}$ contribution shows less pronounced asymmetric broadening (e.g., Fig. 2f).

The prismatine spectra at 300 K (except no. 5) differ from the kornerupine (sensu stricto) spectra in that a distinct shoulder near $-0.5$ and 3.0 mm/s is present. This shoulder could be successfully included into the calculated spectra by splitting the doublet for $Fe^{2+}$ at the X site. The additional absorption is attributed to F $\rightarrow$ OH substitution at the O10 site (see below).

### Variations in the spectra with temperature

Changes in the kornerupine spectra with temperature are distinctive. In contrast to what is frequently observed in other silicates (e.g., Amthauer et al. 1976 for garnets, Redhammer 1996 for clinopyroxenes), spectral resolution does not increase when the temperature is lowered; instead it decreases for kornerupine. Due to the strong superposition of lines at 77 K, there is less precision in the calculated area-ratios and $^{57}Fe$ hyperfine parameters, whereas separation of the X site from the M-site absorptions increases at 430 K.

Two kornerupines were studied at both 77 and 430 K. There are very pronounced changes in the shape of the spectra for the B-free kornerupine (no. 1) with temperature (Fig. 3). This can be seen in the $Fe^{2+}$ QSD at 430 K (Fig. 3f). The $Fe^{2+}$ components are well-separated from each other at both 300 and 430 K. The temperature dependence of the $Fe^{2+}$ quadrupole splittings (Fig. 4) shows a distinctly smaller decrease of $\Delta E_Q$ from $Fe^{2+}$ at the X site with increasing temperature as compared to $\Delta E_Q$ of $Fe^{2+}$ at the M sites. The small negative slope of the decrease of the X-site $\Delta E_Q$ is a further indication that the doublet arises from $Fe^{2+}$ in a strongly distorted environment. In general, less distorted coordination polyhedra show a larger temperature dependence of the $Fe^{2+}$ quadrupole splitting than more distorted polyhedra. This is due to the increased splitting of electronic energy levels of the $Fe^{2+}$ nucleus with increasing distortion (Van Alboom et al. 1993).

The increase in resolution with increasing temperature is less marked in Waldheim prismatine (Fig. 5) than in B-free kornerupine. The decrease of $\Delta E_Q$ of $^{[X]}Fe^{2+}$ with increasing temperature is more pronounced in Waldheim prismatine than in B-free kornerupine (Fig. 4), and thus the environment of the X site in Waldheim prismatine could be less distorted than that of the X site in the B-free kornerupine. Nonetheless, the decrease of $\Delta E_Q$ for $Fe^{2+}$ at the X sites is less than the decrease for $Fe^{2+}$ at

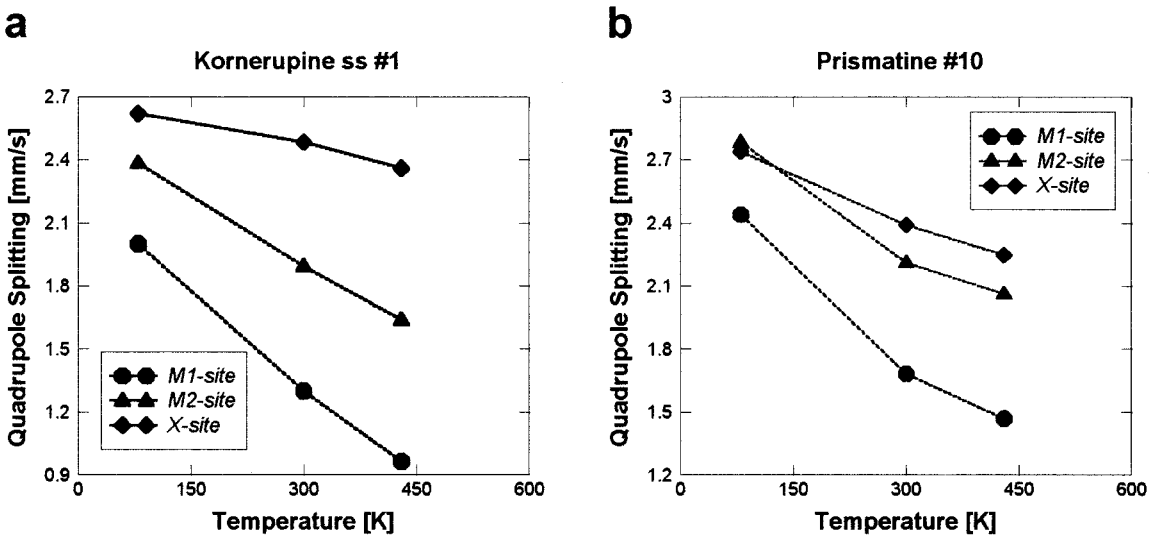


**FIGURE 4.** Variation of $Fe^{2+}$ quadrupole splitting with temperature for B-free kornerupine (no. 1, sample 9365) and for Waldheim prismatine (no. 10, sample P540).

the two M sites, implying that the X polyhedron is less regular than the M polyhedra in Waldheim prismatine.

### Variations in the spectra with chemical composition

Kornerupine-group minerals contain variable amounts of F and B, both of which seem to strongly influence the Mössbauer spectra. Fluorine substitutes for OH at the O10 site, which is bonded to cations at the M1 and X sites. However, because of the marked effect of B on cations at the M1 site, we will consider only the effect of F $\rightarrow$ OH substitution at X, which is distant from the T3 site. Not only is the X-site doublet split in the F-bearing kornerupines, but the proportion of X′, the subsidiary X doublet, increases with F content (Fig. 6), implying that F has an effect on the environment of Fe at the X site.

Substitution of B at the T3 site, with concomitant substitution of Si at the T2 site (Klaska and Grew 1991; Cooper 1997), will affect both the M1 and M2 octahedra, which share corners with T2 and T3; T2 also shares an edge with M1 (Fig. 1). With increasing B content, the M1 and M2 sites seem to become less hospitable to $Fe^{2+}$ relative to Mg, so that the $Fe^{2+}$/Mg ratio in kornerupine decreases relative to the $Fe^{2+}$/Mg ratio in associated ferromagnesian phases (Grew et al. 1990). Although T2 also shares corners with M4, we observed no effect of Al substitution at T2 on the quadrupole splitting of $Fe^{3+}$ at M4. Its quadrupole splitting increases with the relative area of the $Fe^{3+}$ doublet. The quadrupole splitting for $Fe^{2+}$ at M2 increases with B content (Fig. 7), implying that substitution of the small B cation for the larger Si and Al cations increases the distortion of the M2 octahedron. Similarly, the quadrupole splitting of $Fe^{2+}$ at M1 increases with B content (Fig. 8), both for the inner and outer doublets, as does the proportion of the inner doublet (Fig. 9). There are two exceptions to the latter trend, both F-rich: the Waldheim and Port Shepstone prismatines. It is possible that F, which is bound to the M1 cation, is causing the marked deviation of these two samples from the trend set by the other six.

### $Fe^{3+}$ in kornerupine

$Fe^{3+}$ is an important constituent of kornerupine. Wet chemical analysis gave a wide range of $Fe^{3+}/\Sigma Fe$ ratio (i.e., 0 to 1, Hey et al. 1941; McKie 1965; von Knorring et al. 1969; van der Wel 1973), a more extensive range than found in most other rock-forming ferromagnesian silicates. On the basis of pleochroism and of size and distortion of the octahedra, Moore and Araki (1979) suggested that $Fe^{3+}$ occurs only at the M4 site, whereas $Fe^{2+}$ could occur at the M1 and X sites. In refining the structure of ferrian kornerupine from Mautia Hill, Tanzania, Moore et al. (1989) presumed that all Fe at M4 is $Fe^{3+}$, as indicated by wet chemistry. Finger and Hazen (1981) located Fe on the X, M1, M2, and M4 sites in an Fe-rich prismatine from Opinicon Lake, Ontario, but did not mention its oxidation state. Cooper (1997) presumed that Fe at X, M1, and M2 is divalent.

The Mössbauer spectra of kornerupine with $Fe^{3+}/\Sigma Fe < 0.5$ confirm Cooper's (1997) interpretation. The spectra can be fitted with only one $Fe^{3+}$ doublet having hyperfine parameters consistent with octahedral $Fe^{3+}$. If $Fe^{3+}$ were present at a second octahedral site or at a tetrahedral site, the amounts are too small (<2% of total Fe) to be resolved in the spectra of the studied ferroan kornerupines. With one exception, $Fe^{3+}/\Sigma Fe$ ratios determined at 300 K by Mössbauer spectroscopy are in excellent agreement with the crystallographic $^{[M4]}Fe/\Sigma Fe$ ratios (Fig. 10), which were also measured at room temperature (Cooper 1997). The Mössbauer $Fe^{3+}/\Sigma Fe$ ratios tend to increase

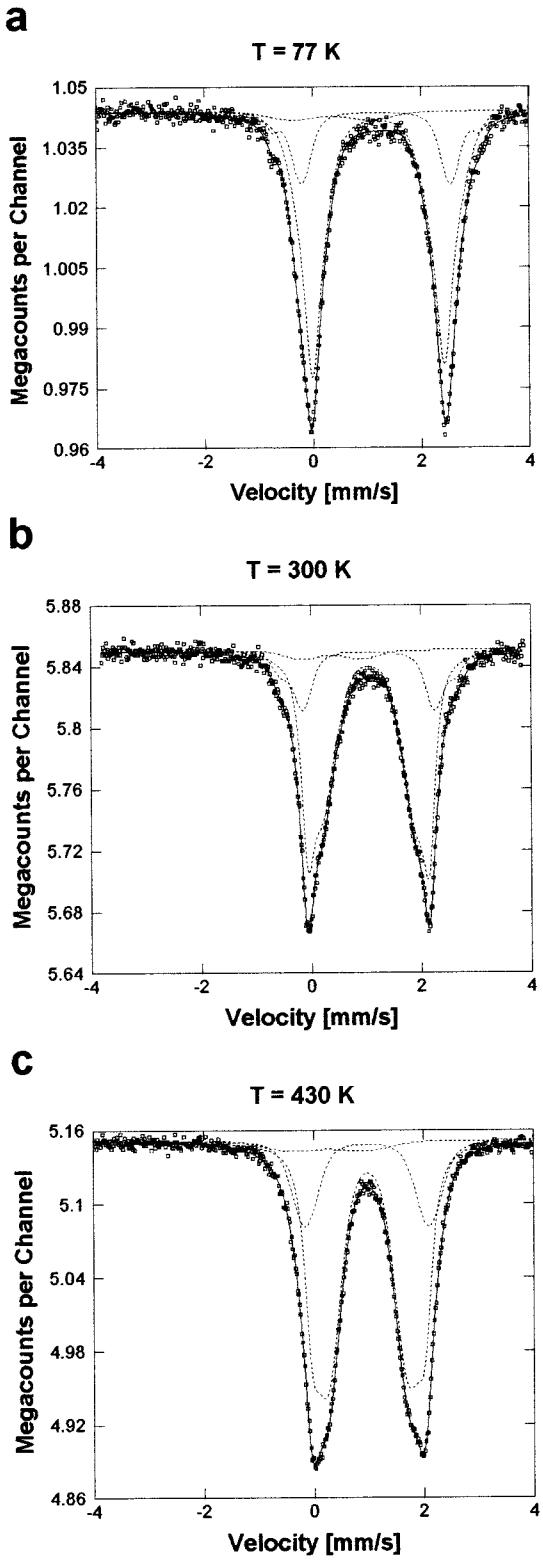


**FIGURE 5.** $^{57}$Fe Mössbauer spectra at 77, 300, and 430 K of the Waldheim prismatine (no. 10, sample P540).

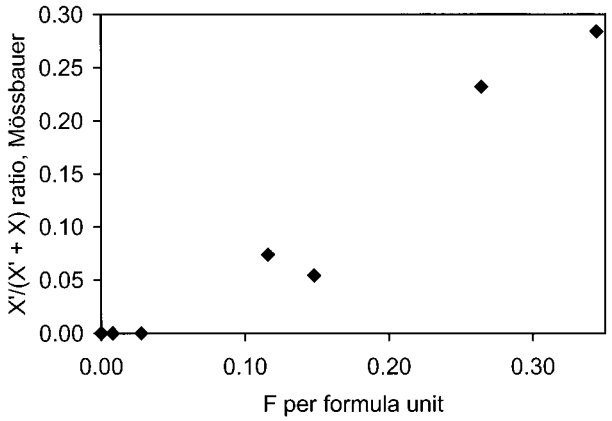


**FIGURE 6.** Relative area of the split-X doublet (X′) to the total area of the X doublet at 300 K as a function of F in kornerupine.

with the temperature at which the spectra were taken, which probably results from the difference in recoil-free fractions of $Fe^{2+}$ and $Fe^{3+}$.

The $Fe^{3+}/\Sigma Fe$ ratio in kornerupine should increase with increasing oxygen fugacity of the environment in which it crystallized. Several minerals associated with kornerupine are useful for qualitatively estimating $f_{O_2}$, and thus could be used to test this premise. Graphite indicates relatively low $f_{O_2}$, whereas the $Fe^{3+}$ contents of sillimanite and the $Fe^{3+}/\Sigma Fe$ ratios of sapphirine and ilmenite-hematite increase with increasing $f_{O_2}$ (e.g., Thompson 1972; Rumble 1976; Grew 1980; Christy 1989). Table 6 lists all samples in which (1) the $Fe^{3+}/\Sigma Fe$ ratio has been determined in kornerupine by SREF, Mössbauer spectroscopy, or by wet chemistry backed at least by preliminary SREF data, and (2) analyses have been reported for associated sillimanite, sapphirine, or ilmenite-hematite. When available, the tabulated data are for associated minerals from

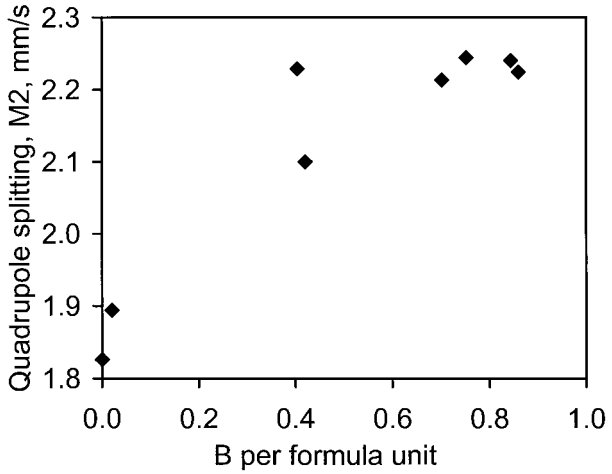


**FIGURE 7.** Variation of the quadrupole splitting of the M2 doublet (millimeters per second) at 300 K with B content in kornerupine.

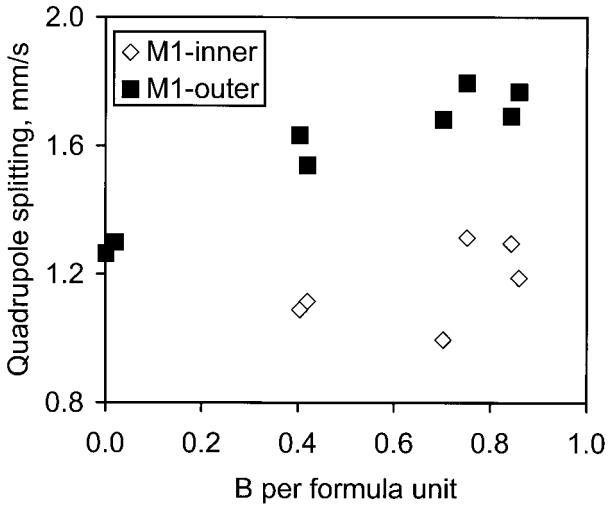


**FIGURE 8.** Variation of the quadrupole splitting (millimeters per second) of the inner and outer M1 doublets at 300 K with B content in kornerupine.

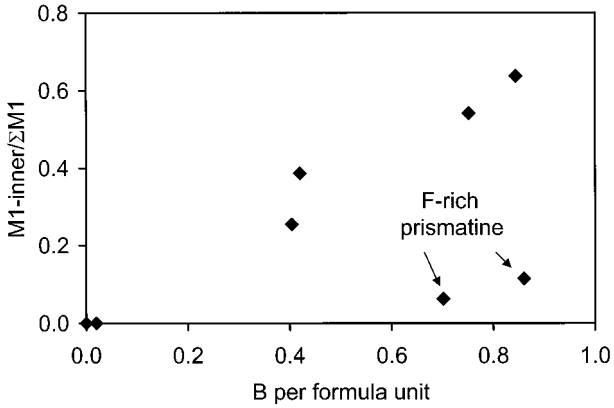


**FIGURE 9.** Relative area of the split M1 doublet (M1-inner) to the total area of the M1 doublet at 300 K as a function of B in kornerupine.

the same sample. If no such data are available and the kornerupine-bearing rocks form small bodies in which there is evidence for relatively constant $f_{O_2}$, then data are given on different samples from the one locality. Port Shepstone, Mase Mountain, and Waldheim meet these criteria (Grew 1986; Grew et al. 1990; Young 1995).

Only two kornerupines among the poorest in $Fe^{3+}$ are found with graphite. Table 6 and Figures 11 and 12 show that, to a first approximation, the $Fe^{3+}/\Sigma Fe$ ratio and $Fe_2O_3$ contents of the associated minerals increase together. The sapphirine data are scattered (Fig. 11). One problem is the relatively large error in calculating $Fe^{3+}/\Sigma Fe$ ratio in sapphirine by stoichiometry. Christy (1989) estimated a standard deviation of 0.026 $Fe^{3+}$ apfu on multiple measurements on a single sample, i.e., 10% in $Fe^{3+}/\Sigma Fe$ ratio in an Fe-poor sapphirine with $\Sigma Fe = 0.26$ apfu. A second, and probably more serious, problem is that the analyzed minerals did not equilibrate. In samples 1 and 2 from Sinyoni Claims, sapphirine formed from kornerupine breakdown and kornerupine margins in contact with the secondary sapphirine has a higher $\Sigma Fe/Mg$ ratio than kornerupine in the core (Schreyer and Abraham 1976). The samples studied by Mössbauer spectroscopy were separated from the cores. It is possible that the kornerupine margins have a higher $Fe^{3+}/\Sigma Fe$ ratio than the cores, so that comparison of kornerupine $Fe^{3+}/\Sigma Fe$ ratio with sapphirine $Fe^{3+}/\Sigma Fe$ ratio would not be valid. A similar explanation may explain the marked discrepancy in sample XF-4 (Reynolds Range, Australia) in which sapphirine also formed from kornerupine breakdown (Vry and Cartwright 1994). Consequently, these three cases have not been plotted in Figure 11.

The sillimanite data are more regular (Fig. 12); only two samples deviate from a clear trend set by the others, no. 8497 (Sinyoni Claims) and 3083E (Ellammankovilpatti, India). The systematic increase of kornerupine $Fe^{3+}$ content with sillimanite $Fe^{3+}$ content is good evidence that kornerupine $Fe^{3+}$ content is, in most cases, an equilibrium feature. One possible explanation for the deviation of 3083E is that during oxidation on the retrograde path (Grew et al. 1987a), $Fe^{2+}$ was oxidized to $Fe^{3+}$ in kornerupine whereas sillimanite was unaffected.

## CONCLUSION

The present work shows the difficulty in locating Fe in a mineral as complicated as kornerupine on the basis of Mössbauer spectroscopy alone. Iron occupies 3 sixfold-coordinated sites and one eightfold-coordinated site, and occurs in both valence states. Moreover, the hyperfine parameters for $Fe^{2+}$ at the eightfold-coordinated site are similar to those of $Fe^{2+}$ at octahedrally coordinated sites. Additional complexities arise from substitutions of F for OH and of B for Si or Al that result in splitting of peaks in the Mössbauer spectra. Only site populations deter-

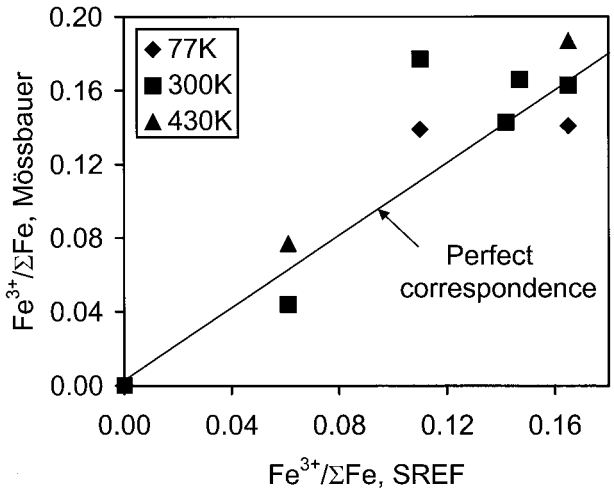


**FIGURE 10.** Comparison of the $Fe^{3+}/\Sigma Fe$ ratio determined by Mössbauer spectroscopy to the $Fe^{3+}/\Sigma Fe$ ratio determined by SREF in kornerupine.

**TABLE 6.** Chemical features of minerals associated with kornerupine of known $Fe^{3+}$ content, listed in order of increasing kornerupine $Fe^{3+}/\Sigma Fe$ ratio

| Locality | Original no. | Cooper no. | Krn SREF $Fe^{3+}/\Sigma Fe$ | Sil, Ky average $Fe^{3+}$, pfu | Spr $Fe^{3+}/\Sigma Fe$ | Ilm or Hem $Fe^{3+}/\Sigma Fe$ | Sources of compositional and petrologic data (see also notes below) |
|---|---|---|---|---|---|---|---|
| Port Shepstone | BM1940,39 | K11 | 0 | (0.006) | — | 0 | Graphite. Grew et al. (1990) |
| Waldheim | — | K20, 24, 34 | 0.003 | (0.007) | (0.034) | — | Grew (1986), Grew and Rossman (1985) |
| Mase Mountain, N.J., U.S.A. | T-8 | K42 | 0.02 | (0.009) | — | (0) | (Graphite). Young (1995) |
| Sinyoni Claims | 9371 | — | 0.03* | — | 0.02–0.56 | — | Schreyer and Abraham (1976) |
| Sinyoni Claims | 8497 | K22 | 0.06 | 0.002 | — | — | This paper, Schreyer and Abraham (1976) |
| Usmun R., Yakutia, Russia | 142-1C | K29 | 0.09 | — | 0.13 | — | Grew et al. (1991) |
| Usmun R., Yakutia, Russia | 134H | K13 | 0.10 | — | 0 | — | Grew et al. (1991) |
| Madagascar | 141255 | K9 | 0.11 | — | 0.12–0.25 | — | Grew et al. (1990) |
| Kondapalle, India | J-21 | K3 | 0.13 | 0.028 | — | H | Grew and Hinthorne (1983) |
| Ellammankovilpatti | 3083D | K1 | 0.15 | 0.016 | — | — | Grew and Hinthorne (1983), Grew et al. (1990) |
| Madagascar | BM1972,170 | K28 | 0.16 | — | 0.29 | — | Grew et al. (1990) |
| Paderu, India | E2724 | K33 | 0.16 | 0.026 | 0.24 | — | Grew and Hinthorne (1983), Grew et al. (1990) |
| Sinyoni Claims | 9365 | K35 | 0.17 | — | 0.37 | — | Schreyer and Abraham (1976) |
| Opinicon Lake, Ont., Canada | OP/WP-109-77 | — | 0.18 | 0.032 | — | 0.13 | H in Ilm. Grew and Hinthorne (1983), Lonker (1988), Grew et at. (1990) |
| Ellanmmankovilpatti | 3083E | K21 | 0.19 | 0.016 | — | — | Grew et al. (1987a) |
| Namaqualand, South Africa | DWN138 | K27 | 0.20 | — | 0.41 | — | Waters and Moore (1985) |
| Fiskenæsset, Greenland | 31498 | K12 | 0.22 | — | 0.09–0.4 | — | Grew et al. (1987b) |
| Labwor, Uganda | PHN984 | K26 | 0.23 | 0.032 | 0.31 | — | Nixon et al. (1984) |
| Reynolds Range, Australia | XF-4 | K36 | 0.31 | — | 0 | — | Vry and Cartwright (1994) |
| Chilapila Hill, Zambia | 8HC161 | K53 | 0.47 | 0.019† | — | 1.00 | Grew et al. (1998) |
| Bjordam, Norway | 128415 | K4 | (0.94)‡ | — | — | 1.00 | van der Wel (1973), Grew et al. (1990) |
| Mautia Hill, Tanzania | D683 | K44 | 1.0‡ | 0.013† | — | 1.00 | McKie (1965), Grew et al. (1990) |

*Note:* () indicates data obtained on other samples from the same locality. Mineral abbreviations: Ky-kyanite, H-hematite lamellae in ilmenite, Hem-hematite, Ilm-ilmenite, Sil-sillimanite, Spr-sapphirine. Kornerupine SREF $Fe^{3+}/\Sigma Fe$ ratios are from Cooper (1997) except 8HC 161 (Cooper, unpublished data) and OP/WP-109-77 (Finger and Hazen 1981). Sapphirine and ilmenite $Fe^{3+}/\Sigma Fe$ ratios were calculated from stoichiometry.

* Based on Mössbauer spectroscopy (Table 4).

† For kyanite.

‡ From wet-chemical data, which are consistent with Moore et al.'s (1989) SREF data on D683 and Cooper's unpublished data on 128415 and other samples from Bjordam.

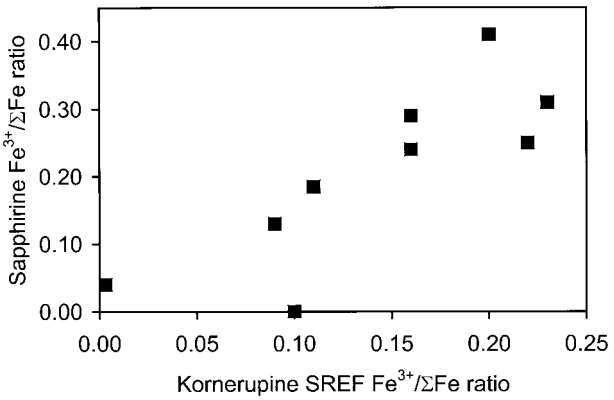


**FIGURE 11.** Comparison of kornerupine $Fe^{3+}/\Sigma Fe$ ratio (as determined by single-crystal structure refinements) with the $Fe^{3+}/\Sigma Fe$ ratio in associated sapphirine. Averages are plotted when a range is given.

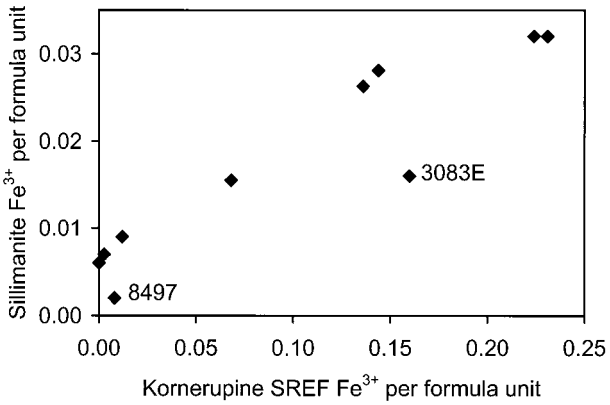


**FIGURE 12.** Comparison of kornerupine $Fe^{3+}$ content (as determined by single-crystal structure refinements) with $Fe^{3+}$ content of associated sillimanite. Averages are plotted when a range is given.

mined by SREF on the same samples allowed us to develop models for refining the Mössbauer spectra and assigning doublets to Fe at specific sites in the structure. The regular increase in $Fe^{3+}$ content of kornerupine (as determined by SREF and Mössbauer spectroscopy) with that in associated minerals is related to the conditions of oxygen fugacity under which the assemblage crystallized.

## Acknowledgments

We thank the Alexander von Humboldt-Stiftung for support of E.S.G.'s research in 1983–1984 when he was a Humboldt Fellow at the Ruhr-Universität Bochum and for support of G.J.R.'s research in 1998. G.J.R. is currently a Humboldt Fellow at Institute of Crystallography at the Rheinisch Westfaelisch Technische Hochschule Aachen. We also thank the University of Salzburg for support of E.S.G.'s stay in 1993 under the cooperative agreement between the University of Salzburg and the University of Maine. F.C.H. and M.A.C. were supported by the National Science and Engineering Research Council of Canada (grants to F.C.H.). The following institutions and individuals generously provided samples: British Museum-Natural History (Natural History Museum) for BM1940,39; Muséum National d'Histoire Naturelle for 171.350; National Museum of Natural History, Smithsonian Institution for 141255; Mineralogical Museum in Saarbrücken for samples from Waldheim (P540) and Lac Ste. Marie (P539); and W. Schreyer for 9365, 8497, and 9371 from Sinyoni Claims. We also thank W. Schreyer for background information and discussion on the Sinyoni Claims samples. We are grateful to M. Bernroider for electron-microprobe analyses of sample 5, Ron Chapman for electron-microprobe analyses of sample 10, Martin Yates for electron-microprobe data on sample 4, and Charles Shearer and Michael Wiedenbeck for assistance in obtaining SIMS analyses of sample 10. We thank Eddy De Grave, Kiyotaka Ishida, David Jenkins, and George Rossman for their comments on earlier drafts of this paper.

## References cited

Amthauer, G., Annersten H., and Hafner, S.S. (1976) The Mössbauer spectrum of $^{57}Fe$ in silicate garnets. Zeitschrift für Kristallographie, 143, 14–55.

Christy, A.G. (1989) The effect of composition, temperature and pressure on the stability of the 1Tc and 2M polytypes of sapphirine. Contributions to Mineralogy and Petrology, 103, 203–215.

Cooper, M.A. (1997) The crystal chemistry of kornerupine, 199 p. M.S. thesis, University of Manitoba, Winnipeg, Canada.

de Villiers, J.E. (1940) Iron-rich kornerupine from Port Shepstone, Natal. Mineralogical Magazine, 25, 550–556.

Dyar, M.D. and Burns, R.G. (1986) Mössbauer spectral study of ferruginous one-layer trioctahedral micas. American Mineralogist, 71, 955–965.

Finger, L.W. and Hazen, R.M. (1981) Refinement of the crystal structure of an iron-rich kornerupine. Carnegie Institution of Washington Year Book, 80, 370–373.

Grew, E.S. (1980) Sillimanite and ilmenite from high-grade metamorphic rocks of Antarctica and other areas. Journal of Petrology, 21, 39–68.

———(1982) Sapphirine, kornerupine, and sillimanite + orthopyroxene in the charnockitic region of South India: Journal of the Geological Society of India, 23, 469–505.

———(1986) Petrogenesis of kornerupine at Waldheim (Sachsen), German Democratic Republic. Zeitschrift für geologische Wissenschaften, 14, 525–558.

———(1996) Borosilicates (exclusive of tourmaline) and boron in rock-forming minerals in metamorphic environments. In Mineralogical Society of America Reviews in Mineralogy, 33, 387–502.

Grew, E.S. and Hinthorne, J.R. (1983) Boron in sillimanite. Science, 221, 547–549.

Grew, E.S. and Rossman, G.R. (1985) Co-ordination of boron in sillimanite. Mineralogical Magazine, 49, 132–135.

Grew, E.S., Abraham, K., and Medenbach, O. (1987a) Ti-poor hoegbomite in kornerupine-cordierite-sillimanite rocks from Ellammankovilpatti, Tamil Nadu, India. Contributions to Mineralogy and Petrology, 95, 21–31.

Grew, E.S., Herd, R.K., and Marquez, N. (1987b) Boron-bearing kornerupine from Fiskenæsset, West Greenland: a re-examination of specimens from the type locality. Mineralogical Magazine, 51, 695–708.

Grew, E.S., Chernosky, J.V., Werding, G., Abraham, K., Marquez, N., and Hinthorne, J.R. (1990) Chemistry of kornerupine and associated minerals, a wet chemical, ion microprobe, and X-ray study emphasizing Li, Be, B and F contents. Journal of Petrology, 31, 1025–1070.

Grew, E.S., Yates, M.G., Beryozkin, V.I., and Kitsul, V.I. (1991) Kornerupine in the slyudites from the Usmun River Basin in the Aldan Shield. 2. Chemistry of the minerals, mineral reactions. Geologiya i Geofizika, 1991(7), 99–116 (in Russian). English translation, Soviet Geology and Geophysics, 32(7), 85–98).

Grew, E.S., Cooper, M.A., and Hawthorne, F.C. (1996) Prismatine: revalidation for boron-rich compositions of the kornerupine group. Mineralogical Magazine, 60, 483–491.

Grew, E.S., Pertsev, N.N., Vrána, S., Yates, M.G., Shearer, C.K., and Wiedenbeck, M. (1998) Kornerupine parageneses in whiteschists and other magnesian rocks: is kornerupine + talc a new high-pressure assemblage equivalent to tourmaline + orthoamphibole? Contributions to Mineralogy and Petrology, 131, 22–38.

Hawthorne, F.C. (1988) Mössbauer spectroscopy. In Mineralogical Society of America Reviews in Mineralogy, 18, 255–340.

Hey, M.H., Anderson, B.W., and Payne, C.J. (1941) Some new data concerning kornerupine and its chemistry. Mineralogical Magazine, 26, 119–130.

Klaska, R. and Grew, E.S. (1991) The crystal structure of boron-free kornerupine: Conditions favoring the incorporation of variable amounts of B through $^{[4]}B \leftrightarrow {}^{[4]}Si$ substitution in kornerupine. American Mineralogist, 76, 1824–1835.

Lonker, S.W. (1988) An occurrence of grandidierite, kornerupine, and tourmaline in southeastern Ontario, Canada. Contributions to Mineralogy and Petrology, 98, 502–516.

McKie, D. (1965) The magnesium aluminium borosilicates: kornerupine and grandidierite. Mineralogical Magazine, 34, 346–357.

Moore, P.B. and Araki, T. (1979) Kornerupine: a detailed crystal-chemical study. Neues Jahrbuch für Mineralogie Abhandlungen, 134, 317–336.

Moore, P.B. and Bennett, J.M. (1968) Kornerupine: Its crystal structure. Science, 159, 524–526.

Moore, P.B., Sen Gupta, P.K., and Schlemper, E.O. (1989) Kornerupine: Chemical crystallography, comparative crystallography, and its cation relation to olivine and to $Ni_2In$ intermetallic. American Mineralogist, 74, 642–655.

Nixon, P.H., Grew, E.S., and Condliffe, E. (1984) Kornerupine in a sapphirine-spinel granulite from Labwor Hills, Uganda. Mineralogical Magazine, 48, 550–552.

Ping, J.Y., Rancourt, D.G., and Stadnik, Z.M. (1991) Voigt-based methods for arbitrary-shape quadrupole splitting distributions (QSD′s) applied to quasi-crystals. Hyperfine Interactions, 69, 493–496.

Rancourt, D.G. and Ping, J.Y. (1991) Voigt-based methods for arbitrary-shape static hyperfine parameter distributions in Mössbauer spectroscopy. Nuclear Instruments and Methods in Physics Research, B58, 85–97.

Rancourt, D.G., Ping, J.Y., and Berman, R.G. (1994a) Mössbauer spectroscopy of minerals III. Octahedral-site $Fe^{2+}$ quadrupole splitting distributions in the phlogopite-annite series. Physics and Chemistry of Minerals, 21, 258–267.

Rancourt, D.G., Christie, I.A.D., Royer, M., Kodama, H., Robert, J.-L., Lalonde, A.E., and Murad, E. (1994b) Determination of accurate $^{[4]}Fe^{3+}$, $^{6}Fe^{3+}$, and $^{6}Fe^{2+}$ site populations in synthetic annite by Mössbauer spectroscopy. American Mineralogist, 79, 51–62.

Rancourt, D.G., Ping, J.Y., Boukili, B., and Robert, J.-L. (1996) Octahedral-site $Fe^{2+}$ quadrupole splitting distributions from Mössbauer spectroscopy along (OH, F)-annite join. Physics and Chemistry of Minerals, 23, 63–71.

Redhammer, G.J. (1996) Untersuchungen zur Kristallchemie und Kristallphysik von synthetischen Klinopyroxenen im System Hedenbergit–Akmit $CaFe^{2+}\{Si_2O_6\}$–$NaFe^{3+}\{Si_2O_6\}$, 201 p. Ph.D. dissertation, Universität Salzburg.

———(1998) Characterisation of synthetic trioctahedral micas by Mössbauer spectroscopy. In D.G. Rancourt, Ed., Mössbauer spectroscopy in Clay Science, ICC '97 special issue. Hyperfine Interactions, 117, in press.

Rumble, D. III (1976) Oxide minerals in metamorphic rocks. In Mineralogical Society of America Reviews in Mineralogy, 3, R-1–R-24.

Schreyer, W. and Abraham, K. (1976) Natural boron-free kornerupine and its breakdown products in a sapphirine rock of the Limpopo Belt, southern Africa. Contributions to Mineralogy and Petrology, 54, 109–126.

Thompson, J.B. Jr. (1972) Oxides and sulfides in regional metamorphism of pelitic schists. 24th International Geological Congress, Montreal, Section 10, 27–35.

Van Alboom, A., De Grave, E., and Vandenberghe, R.E. (1993) Study of the temperature dependence of the hyperfine parameters in two orthopyroxenes by $^{57}$Fe Mössbauer spectroscopy. Physics and Chemistry of Minerals, 20, 263–275.

van der Wel, D. (1973) Kornerupine: a mineral new to Norway. Contribution to the mineralogy of Norway, no. 53. Norsk Geologisk Tidsskrift, 53, 349–357.

von Knorring, O., Sahama, T.G., and Lehtinen, M. (1969) Kornerupine-bearing gneiss from Inanakafy near Betroka, Madagascar. Bulletin of the Geological Society of Finland, 41, 79–84.

Vry, J.K. and Cartwright, I. (1994) Sapphirine-kornerupine rocks from the Reynolds Range, central Australia: constraints on the uplift history of a Proterozoic low pressure terrain. Contributions to Mineralogy and Petrology, 116, 78–91.

Waters, D.J. and Moore, J.M. (1985) Kornerupine in Mg—Al-rich gneisses from Namaqualand, South Africa: mineralogy and evidence for late-metamorphic fluid activity. Contributions to Mineralogy and Petrology, 91, 369–382.

Young, D.A. (1995) Kornerupine-group minerals in Grenville granulite-facies paragneiss, Reading Prong, New Jersey. Canadian Mineralogist, 33, 1255–1262.

Manuscript received May 4, 1998
Manuscript accepted October 16, 1998
Paper handled by David M. Jenkins

View publication stats